Macromolecules
ARTICLE

Macromolecules **2010**, *43*, 3549–3555 **3549**
DOI: 10.1021/ma1000354

Phase Behavior of Asymmetric Multicomponent A/B/A−C Blends with Unequal Homopolymer Molecular Weights

Alisyn J. Nedoma,[†] Peggy Lai,[†] Andrew Jackson,[‡,§] Megan L. Robertson,[⊥] Nisita S. Wanakule,[†] and Nitash P. Balsara*[,†,∥,#]

[†]*Department of Chemical Engineering, University of California, Berkeley, California 94720,* [‡]*National Institute of Standards and Technology Center for Neutron Research, Gaithersburg, Maryland, 20899,* [§]*Department of Materials Science and Engineering, University of Maryland, College Park, Maryland 20742,* [⊥]*Department of Chemical Engineering and Materials Science, Minneapolis, Minnesota, 55455,* [∥]*Materials Sciences Division, Lawrence Berkeley National Laboratory, Berkeley, California 94720, and* [#]*Environmental Energy Technologies Division, Lawrence Berkeley National Laboratory, Berkeley, California 94720*

Received January 6, 2010; Revised Manuscript Received March 3, 2010

ABSTRACT: Small angle neutron scattering is used to study the phase behavior of mixtures of two immiscible homopolymers (A and B) and a diblock copolymer (A−C) wherein B and C chains exhibit attractive interactions (negative Flory−Huggins interaction parameter) and the other pairs of chains exhibit repulsive interactions. This study explores the effect of homopolymer molecular weight asymmetry ($N_A/N_B \neq 1$, where N_I is the number of monomer units per chain in homopolymer I) at fixed segregation strength of the homopolymers. The temperature windows over which lamellae, microemulsions, macrophase separation, and homogeneous phases are found are affected qualitatively by N_A/N_B. In particular, a homogeneous window that was not present in symmetric A/B/A−C blends is seen when N_A/N_B exceeds a critical value.

Introduction

This paper is part of a series on mixtures of two immiscible homopolymers (A and B) and a diblock copolymer (A−C) wherein B and C chains exhibit attractive interactions (negative Flory−Huggins interaction parameter) and the other pairs of chains exhibit repulsive interactions.[1−6] Our objective is to obtain a single, thermodynamically stable, microphase separated structure that may lead to improved mechanical properties[7−10] or provide channels for controlling transport through these systems.[11−14] The A/B/A−C blends are thermodynamically analogous to oil/water mixtures stabilized by nonionic surfactants[15−22] wherein the alkyl polyglycol ether portion of the surfactant exhibits attractive interactions with water. Thus, homopolymer A is analogous to oil, homopolymer B is analogous to water, and the A−C diblock copolymer behaves like the nonionic surfactant. Oil/water/surfactant studies have systematically varied the molecular weight of the oil to observe the effect of molecular structure on microstructure formation.[23−25] In these studies, the molecular weight of the hydrophilic phase is invariant because water is used. A/B/A−C polymer blends offer the possibility of varying the molecular weights of both homopolymers, the oil- and the water-analogue, providing new insight into the phase behavior of A/B/A−C systems.[1−5,26−30]

Most previous work with ternary polymer blends involves symmetric A-B diblock copolymers that have been added to symmetric mixtures of A and B homopolymers with roughly equal chain lengths (i.e., $N_A/N_B \approx 1$, N_I is the number of monomers in a chain of species I based on a reference volume $v_{ref} = 0.1$ nm^3).[31−51] While there have been no previous studies aimed at a systematic study of the effect of N_A/N_B on thermodynamics, these nominally symmetric studies cover values of N_A/N_B from 0.44 − 2.12.[37,38] In a landmark publication, Bates and co-workers reported the formation of microemulsions in symmetric A/B/A-B blends where $\chi_{AB}N$ for the diblock was around 10.5 and $\chi_{AB}N_A$ was in the vicinity of 2.0 for the binary blend without diblock.[33,42,51−56] These experiments were motivated by elegant theoretical predictions of a Lifshitz point in the vicinity of the observed microemulsion.[57−62]

In this paper we explore microstructure formation in A/B/A−C blends where both the diblock copolymer and the binary mixture of homopolymers are near critical conditions. We have chosen to vary the molecular weight asymmetry of the homopolymers (N_A/N_B values range from 0.6 to 18.7) while using a nearly symmetric diblock copolymer ($N_{A,block} = 1509$, $N_{C,block} = 1257$). In all cases, the copolymer is added to binary blends at their critical compositions. The blends in this study are designed to examine the effect of N_A/N_B on blend thermodynamics at fixed segregation strength. To our knowledge, this is the first systematic study of microstructure formation in block copolymer-containing multicomponent mixtures with N_A/N_B values that differ significantly from unity.

Experimental Section

Component A is deuterated polybutadiene with 89% 1,2 monomer addition, component B is polyisobutylene, and component A−C is a linear diblock in which block A is hydrogenated polybutadiene with 89% 1,2 addition and block C is hydrogenated polybutadiene with 63% 1,2 addition. Components A and A−C were synthesized anionically and saturated under high pressure, and component B was synthesized cationically. Both syntheses are described elsewhere.[1] Absolute molecular weights were measured with a Viscotek[63] triple detector array system and Styragel columns on a Waters HPLC with THF as the mobile phase. The fraction of 1,2-monomer addition for components A and A−C was measured using H NMR spectroscopy. Deuteration levels in component A were measured using a

*To whom correspondence should be addressed. E-mail: nbalsara@berkeley.edu. Telephone: 510.642.8937. Fax: 510.642.4778.

Published on Web 03/12/2010

Table 1. Polymer Characteristics

polymer species	name	M_w (kg/mol)[a]	PDI[a]	ρ (g/cm^3) (at 23 °C)[b]	n_D[b]	used in blend
dPBD	A1	25.3	1.01	0.9070	2.79	TB0.6, STB2
dPBD	A2	50.9	1.02	0.9046	2.63	STB4
dPBD	A3	62.3	1.01	0.9031	2.52	STB5
dPBD	A4	69.9	1.02	0.9183	3.49	TB4
dPBD	A5	230	1.02	0.9032	2.62	TB19
PIB	B1	12.5	1.04	0.9134		TB19
PIB	B2	18.7	1.02	0.9131		TB4
PIB	B3	24.0	1.05	0.9131		STB2
PIB	B4	42.5	1.02	0.9135		TB0.6
PIB	B5	44.6	1.04	0.9140		STB4
PIB	B6	56.8	1.02	0.9144		STB5
hPBD−hPBD	AC	78.5−65.4	1.01	0.8639		all

[a] M_w and PDI are measured by GPC. [b] ρ, the density, and n_D, the average number of deuterium atoms per C_4H_8 repeat unit, are measured using a density gradient column.

density gradient column. The characteristics of the polymers used in this study are summarized in Table 1. The Flory−Huggins χ interaction parameters were obtained from fits of the random phase approximation to SANS profiles from binary blends within the homogeneous window. The temperature dependences of χ_{AB} and χ_{AC} are reported in ref 29 and the temperature, composition, and molecular weight dependence of χ_{BC} is reported in ref 64.

Blend components were dissolved in hexane, partially dried under nitrogen, and precipitated in a 1:1 methanol/acetone mixture. Ultrahigh purity (>99.9%) solvents were used for all steps. The precipitated samples were transferred to a 1 mm-thick annular aluminum spacer with inner diameter 17 mm, placed on a 1 mm-thick quartz disk, and dried under vacuum for 2 days. The temperature of the vacuum oven was raised to 90 °C and the samples were heated under vacuum for an additional day. A second piece of quartz was pressed onto the samples while they were slightly warm (~40 °C), and the perimeter of the sample was sealed with heat-proof epoxy, except for a 5 mm gap that was left open to allow the polymer to expand when heated. The samples were annealed in the oven upright, with the gap at the top (this is the orientation in which it was placed in the SANS beamline), under vacuum at 90 °C for 1 h.

Small angle neutron scattering (SANS) measurements were made at the NG3 beamline at the National Institute of Standards and Technology Center for Neutron Research in Gaithersburg, Maryland. All samples were heated from 30 − 90 °C in 10 °C increments, and from 90 − 190 °C in 20 °C increments. One of the samples (TB0.6) was heated a second time from 110 to 130 °C in 2 °C increments to resolve the location of a phase transition. The SANS data from TB0.6 obtained at 100 °C in the 20 °C increment run was identical to that obtained in the 2 °C increment run. The samples were annealed for at least 10 min after each change in temperature. In regimes where microphase separated states were observed the scattering profiles obtained immediately after the temperature step were identical to those obtained following a 10 min anneal. In regimes where macrophase separation was observed, SANS profiles obtained after 10 min were slightly different from the early time data due to coarsening. On the basis of these observations and our previous experience with the blend system studied here,[1,3−5,29] we conclude that our protocols enable us to determine the equilibrium structure of our A/B/A−C blends. SANS profiles, collected in 5 min acquisition intervals, were corrected for background, empty cell, transmission, incoherent scattering, due to nonuniformity in deuteration, and the data were integrated azimuthally to render I vs q profiles ($q = 4\pi \sin(\theta/2)/\lambda$ in which θ is the scattering angle and λ is the wavelength of incident neutrons).[1,65]

Results and Discussion

Expressions for the Flory−Huggins interactions parameters, χ_{AB}, χ_{AC}, and χ_{BC} are given in a footnote[66] based on previous studies of binary A/B, A/C, and B/C blends.[3,64] The study is restricted to blends of polymers with critical composition calculated using the Flory−Huggins theory[67,68] (on a block copolymer-free basis):

$$\phi_{A,crit} = \frac{1}{1 + (N_A/N_B)^{1/2}} \quad (1)$$

While varying N_A/N_B over two decades (consequently varying $\phi_{A,crit}$), we hold fixed the segregation strength of the A/B homopolymers, given as the product of the Flory−Huggins interaction parameter, χ_{AB}, and N_{AVE}:

$$N_{AVE} = 4\left[\frac{1}{N_A^{1/2}} + \frac{1}{N_B^{1/2}}\right]^{-2} \quad (2)$$

$N_{AVE} \cong 588$ for each of the three asymmetric blends studied, yielding $\chi_{AB}N_{AVE}$ values that range from 2.6 to 3.0. The nearly symmetric diblock copolymer used in this study has $\chi_{AC}N$ that ranges from 8.4 to 19 in the experimental temperature window 30 - 190 °C. The neat diblock copolymer exhibited an order-to-disorder (ODT) transition at 140 ± 10 °C. The predicted ODT for the copolymer, based on χ_{AC} reported in ref 3 is 128 °C. In this initial study, we restrict our attention to blends with 40 vol % of the diblock copolymer. The blend characteristics are summarized in Table 2. Blends are identified by the nominal value of N_A/N_B, e.g. TB19 corresponds to the A/B/A−C ternary blend with $N_A/N_B = 18.7$. We compare results obtained from the asymmetric blends with those of three previously studied symmetric blends[29] that contain the same diblock copolymer at the same concentration and encompass $\chi_{AB}N_{AVE} \cong 2.7$. The characteristics of the symmetric ternary blends are also given in Table 2 with the nomenclature STBx, where x refers to the nominal value of $\chi_{AB}N_{AVE}$ at 30 °C.

Table 2. Blend Characteristics

blend	constituents	N_A[a]	N_B	$\phi_{A,crit}$	$\phi_{diblock}$[b]	N_A/N_B	$\chi N_{AVE,AB}$
TB19	A5/B1/AC	4237	227	0.188	0.4	18.7	2.66−3.02
TB4	A4/B2/AC	1264	340	0.342	0.4	3.72	2.62−2.97
TB0.6	A1/B4/AC	463	772	0.564	0.4	0.60	2.62−2.97
STB2	A1/B3/AC	463	437	0.493	0.4	1.06	2.00−2.27
STB4	A2/B5/AC	935	811	0.482	0.4	1.15	3.87−4.38
STB5	A3/B6/AC	1146	1032	0.487	0.4	1.11	4.83−5.48

[a] N_A and N_B are the number of reference volume units in a single polymer chain where the volume of a reference unit is 0.1 nm^3. [b] A nearly symmetric diblock copolymer was used in all blends, with $N_{A,block} = 1509$ and $N_{C,block} = 1257$, giving $f_A = 0.55$.

SANS profiles obtained from TB19, shown in Figure 1a, exhibit scattering in two regimes, delineated at 140 ± 10 °C. The scattering profiles below 140 °C exhibit a low-q up-turn that is consistent with the Porod scattering law ($I \sim q^{-4}$), indicating

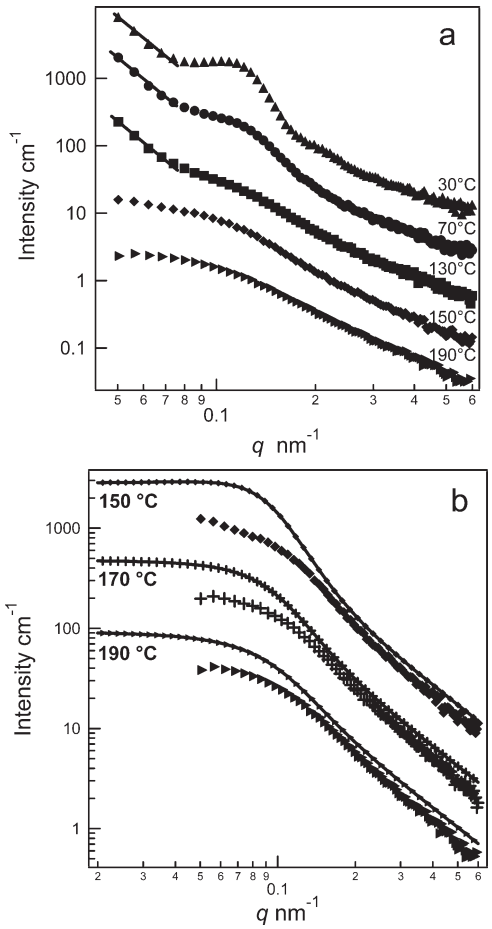

Figure 1. SANS intensity I versus scattering vector q for blend TB19 at selected temperatures. (a) Profiles shifted vertically as follows: 2000 cm^{-1} (30 °C), 1100 cm^{-1} (70 °C), 0 cm^{-1} (130 °C), −1100 cm^{-1} (150 °C), −2000 cm^{-1} (190 °C). The solid lines are power laws with a slope of −4, consistent with Porod scattering. (b) I versus q from homogeneous blends are shown with markers along with the corresponding RPA predictions, shown as lines connecting markers. The SANS and RPA profiles have been shifted as follows: 1000 cm^{-1} (150 °C), 500 cm^{-1} (170 °C), 0 cm^{-1} (190 °C). In this and subsequent SANS profiles, error bars represent ±1 standard deviation. Here the error bars fall within the symbol size.

the presence of strongly segregated interfaces. Following previous studies,[32,69] we take this to be a signature of macrophase separation. The peak in these SANS profiles suggests that one of the macrophases is periodic. Above 140 °C the blend is single phase as indicated by the lack of the low-q up-turn in these data. The SANS profiles from homogeneous blends can be calculated independently using the multicomponent random phase approximation (RPA).[1,70,71] Inputs to the RPA include the binary Flory−Huggins parameters describing monomer−monomer interactions and the statistical segment length of each species (homopolymers and blocks). We use previously published values of these parameters[29,64,66] and established methods[1,70] to predict SANS profiles within the homogeneous window for blend TB19 using no adjustable parameters. The RPA calculations predict continuous profiles for temperatures ≥140 °C. Below 140 °C, the calculated profiles contain a pole at finite q, indicating phase behavior outside of the homogeneous window. Figure 1b shows a comparison between RPA predictions and experiment. Many of the important features in the experimental data are captured by the RPA calculations. The $I \sim q^{-2}$ tail at high q is captured quantitatively by RPA, as is the value of q where $I(q)$ turns over and approaches a plateau. The lack of quantitative agreement between the RPA calculations and experimental data in the high q regime indicates that the statistical segment length of at least one of the components is affected by the presence of the other components. In the experiments, the value of the low-q plateau decreases from 110 to 60 cm^{-1} as the temperature is changed from 150 to 190 °C, while in the RPA calculations, the low-q plateau decreases from 170 to 92 cm^{-1} in the same window. The departure between theory and experiment may derive from inaccuracies in the χ parameters used for the calculations. Even in the simple case of binary B/C blends we have shown a significant dependence of χ on N_B/N_C.[64] Given that the parameters used in these calculations were obtained from binary blends where $N_i/N_j \cong 1$, the inconsistency between RPA and measured data is not surprising. The RPA calculations thus provide strong support for the proposed homogeneous phase at temperatures above 140 °C. It is clear, however, that TB19 does not exhibit a single microphase separated phase in the temperature window 30 − 190 °C.

SANS data from blend TB4, shown in Figure 2a (N_A/N_B = 3.72), are qualitatively different from those of TB19 discussed above. At low temperatures, the SANS profiles contain a well-defined scattering peak at $q^* = 0.107$ nm^{-1}, a shoulder at $2q^* = 0.214$ nm^{-1}, and no Porod scattering at low q. In addition, the two-dimensional SANS scattering profiles are azimuthally asymmetric, as shown in Figure 2b and quantified in Figure 2c. (All of the SANS data from TB19 were azimuthally symmetric). The integrated SANS intensity between q = 0.093 and 0.128 nm^{-1} (in the vicinity of the primary peak) was determined as a function of azimuthal angle, α, and the standard deviation of the data set, σ, is taken as a measure of azimuthal asymmetry. The results of this integration at 30 °C are shown in the inset of Figure 2c, giving σ = 169 cm^{-1}. Following previous work,[37] we take the asymmetry to be the signature of an ordered microphase. The azimuthal asymmetry arises due to flow fields created during sample preparation. In Figure 2c, we show the temperature dependence of σ. The value of σ decreases with increasing temperature and approaches the isotropic value of 5.5 at temperatures >120 °C. In a previous study on pure diblock copolymers,[72] the disappearance of azimuthal asymmetry was a signature of the ODT. On the basis of this, we conclude that TB4 undergoes an ODT when heated above 120 ± 10 °C.

In Figure 2d, we show the temperature dependence of the normalized TB4 SANS profiles in the vicinity of the $2q^*$ peaks. The normalized profiles are obtained by dividing the q-dependent scattering intensity at a given temperature with the scattering intensity obtained deep within the disordered state at 190 °C. In previous studies, we have shown that this procedure is a model-free method for accentuating weak higher order peaks in the scattering profiles of polymer samples with accessible disordered states.[36] Our rationale for this normalization is that the structural information contained in the measured scattering profile is convoluted with the form factors of the polymer chains. Dividing out the profile obtained deep in the disordered state removes (or minimizes) the scattering contribution of the form factors, leaving structural scattering to dominate the normalized profile. The normalized profiles shown in Figure 2d were fit to a Gaussian with an exponential baseline to estimate the area under the $2q^*$ peaks, A_2. A sharp decrease in A_2 is seen at 65 ± 5 °C which is 55 °C below the ODT determined by the σ-based approach. The difference can be attributed to the fact that the ability to detect higher order peaks depends on a variety of factors such as the extent of long-range order, the resolution of the scattering instrument (SANS instruments tend to have relatively broad resolution functions), and the scattering contrast between the microphases. There are many examples of pure diblock copolymers that do not show higher order SANS peaks in the ordered state.[73] We have conducted this analysis on numerous sets of

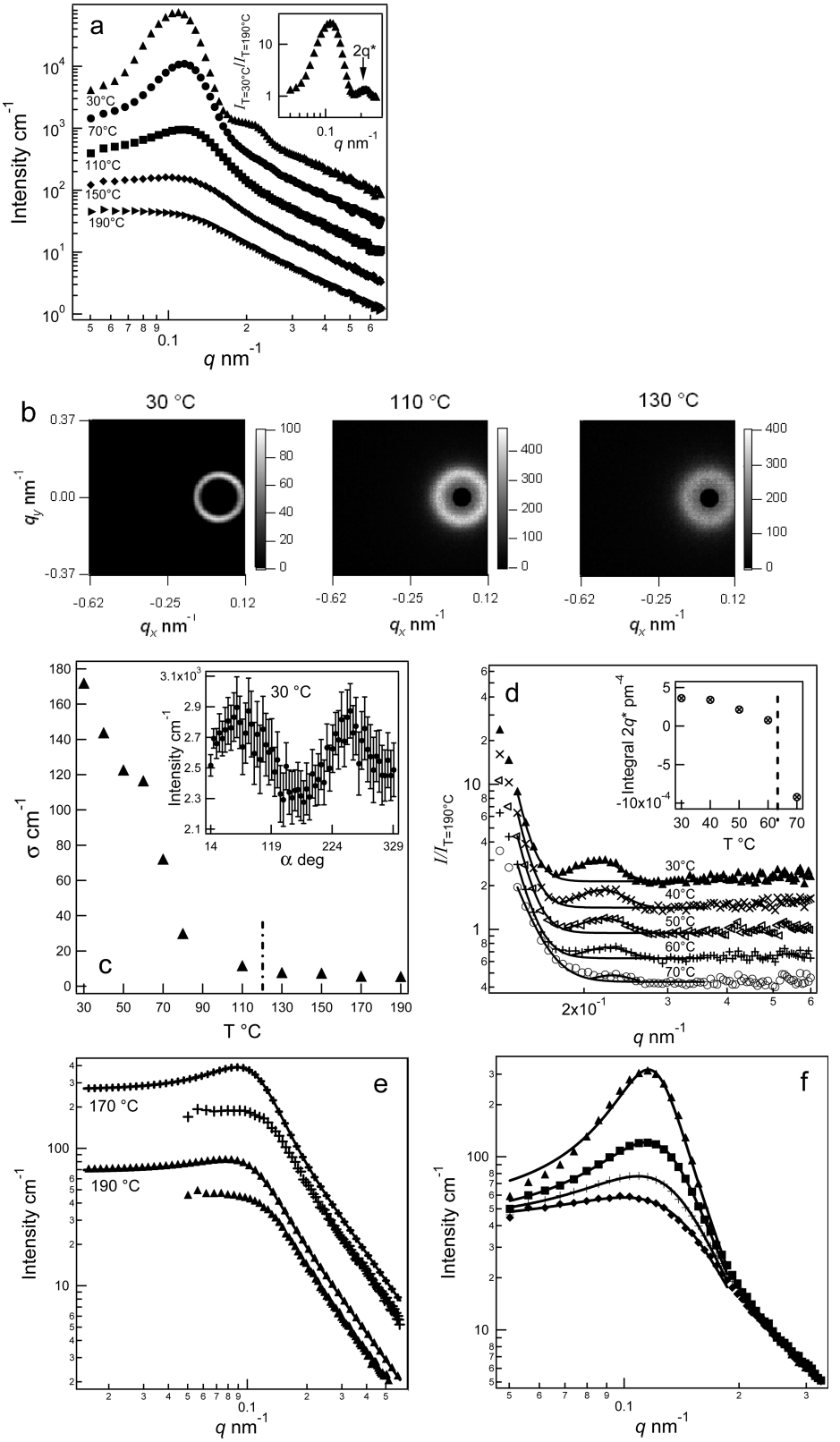

Figure 2. SANS data and analysis for blend TB4. (a) SANS intensity I versus scattering vector q. Profiles shifted vertically as follows: 30100 (30 °C), 22840 (70 °C), 14650 (110 °C), 7120 (150 °C), 0 (190 °C). The inset shows the intensity profile at 30 °C normalized by that at 190 °C. (b) Two dimensional SANS scattering profiles at selected temperatures: deep within the lamellar phase (30 °C), before the loss of azimuthal asymmetry (110 °C), and after the loss of azimuthal asymmetry (130 °C). (c) Azimuthal scattering asymmetry, σ, versus temperature. The dotted line represents the transition between azimuthally asymmetric and symmetric scattering. Inset: Dependence of integrated scattering on azimuthal angle α at 30 °C. (d) Normalized SANS scattering profiles highlighting the $2q^*$ peak with the following vertical shifts: 10 (30 °C), 5 (40 °C), 0 (50 °C), −5 (60 °C), −10 (70 °C). The solid curves are Gaussian fits to the $2q^*$ peak and the exponentially decaying backgrounds. Inset: Integral of the $2q^*$ peak versus temperature. (e) SANS profiles from homogeneous blends at 170 °C (+) and 190 °C (▲) compared with RPA predictions at the same temperatures, shown with lines connecting the markers. The profiles have been shifted as follows: 0 cm^{-1} (170 °C) and 100 cm^{-1} (190 °C). (f) SANS scattering profiles with Teubner−Strey fits to $1q^*$ for the following temperatures: 80 °C (▲), 110 °C (■), 130 °C (+), 150 °C (♦). As in Figure 1, the error bars are less than the symbol size for SANS profiles.

Table 3. Teubner−Strey (TS) Fitting Parameters for Blend TB4 at Select Temperatures

	temperature in °C			
TS parameter	80	110	130	150
a (cm)	0.019	0.023	0.023	0.023
b (cm·nm^2)	−2.39	−2.21	−1.71	−1.20
c (cm·nm^4)	89.3	83.6	71.9	60.6

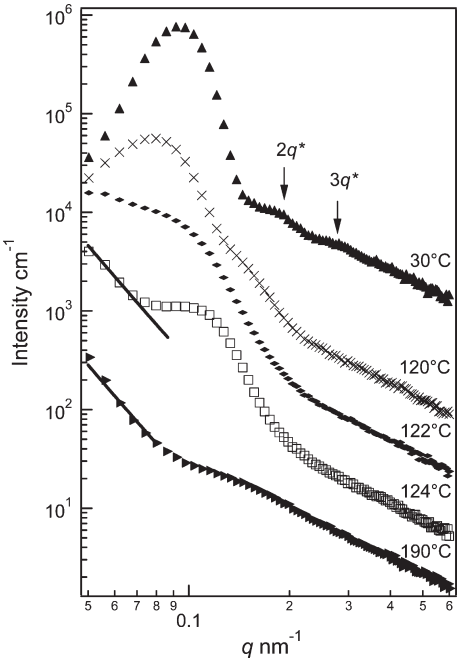

Figure 3. Absolute intensity SANS scattering profiles for blend TB0.6 with the following shifts: 5×10^5 cm^{-1} (30 °C), 3×10^5 cm^{-1} (120 °C), 2×10^5 cm^{-1} (122 °C), 9×10^4 cm^{-1} (124 °C), 0 cm^{-1} (190 °C). Solid lines are power laws with a slope of −4.

SANS data. In all cases, we find that either the A_2- and σ-based estimates of the ODT are in agreement or that the A_2-based estimate lies below that of the σ-based estimate. We thus take the σ-based estimate as the ODT of TB4.

In order to ascertain the nature of the high temperature disordered phase, we carried out multicomponent RPA calculations. These calculations indicated the presence of an homogeneous phase at temperatures above 150 °C, as shown in Figure 2e. As with blend TB19, the RPA and measured SANS profiles agree qualitatively but not quantitatively. The presence of a shallow peak at $q = 0.11$ nm^{-1} in the SANS profiles between 80 and 150 °C suggests the presence of a microphase separated state. Many studies have shown that SANS data from microemulsions can be fit to the Teubner−Strey equation:[18]

$$I = \frac{1}{a + bq^2 + cq^4} \tag{3}$$

The scattering profiles for temperatures 80−150 °C were fitted with the Teubner−Strey equation and the results are shown in Figure 2f. At 80 °C (and below) the low q data are not well fit by the Teubner−Strey equation because the $1q^*$ peak is too sharp, suggesting that the blend is lamellar at these temperatures. The fits from 110 to 150 °C are consistent with the Teubner−Strey equation, supporting the presence of a microemulsion in this temperature window. The fitted values of a, b, and c, summarized in Table 3, are similar to those reported in our previous studies on microemulsions in symmetric A/B/A−C blends.[3,4] The parameter b is negative when fit to the scattering profile of a

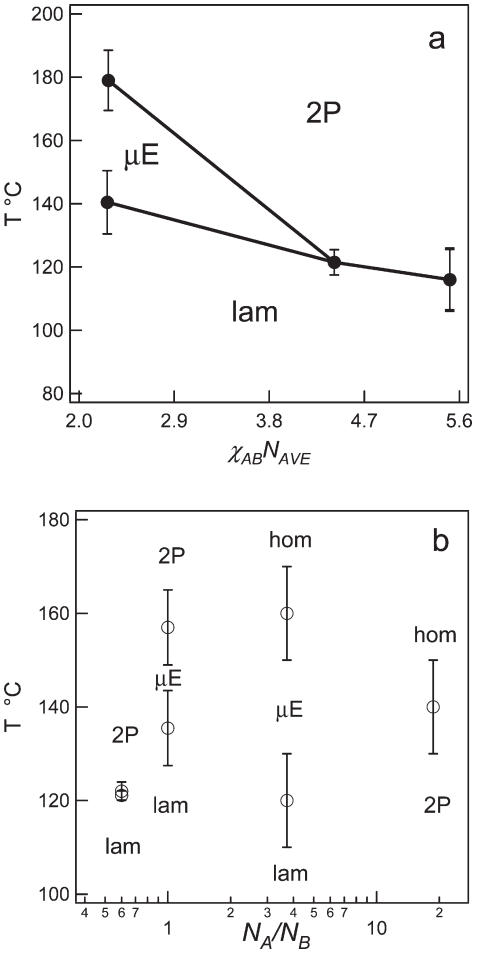

Figure 4. Phase behavior denoted by hom, homogeneous phase; 2P, macrophase separated state; μE, microemulsion; and lam; lamellae. Key: (a) phase transition temperatures as a function of segregation strength, $\chi_{AB}N_{AVE}$, for the symmetric blends (STB series) in Table 2; (b) phase transition temperatures as a function of N_A/N_B (TB series including interpolated data at $N_A/N_B = 1$).

microemulsion, and while b may be negative when fit to other microstructures, a positive value for b unambiguously identifies a structure that is not a microemulsion. The transition from a microemulsion to a homogeneous phase appears to be continuous as the peak at $q = 0.11$ nm^{-1} fades to a monotonic scattering profile upon heating. It is evident that scattering from microemulsions is azimuthally symmetric indicating the presence of randomly oriented microstructrues even though the precursor phase from which it was formed contained a nonrandom collection of lamellar grains. Electron micrographs of lamellar and microemulsion phases formed in polyolefin-based A/B/A−C mixtures are given in ref 2.

The scattering profiles for blend TB0.6 are shown in Figure 3. At low temperatures the blend exhibits peaks at q^*, $2q^*$, and $3q^*$, consistent with a lamellar phase. At 122 ± 2 °C the blend macrophase separates as evidenced by the onset of Porod scattering. As was the case with TB4, the scattering from the lamellar phase is azimuthally asymmetric. The onset of Porod scattering coincides with the temperature at which σ decreases to a constant value for isotropic scattering. RPA calculations for TB0.6 indicate the absence of a homogeneous phase in the 30−190 °C window, consistent with experimental observations.

In Figure 4a, we show the phase behavior of three symmetrical A/B/A−C systems taken from the literature.[3,29] These blends contain the same block copolymer used in the asymmetric blends at the same volume fraction, as given in Table 2. All of the

symmetric blends exhibit a lamellar phase at low temperatures and macrophase separation at high temperatures. STB2 exhibits a microemulsion at intermediate temperatures. The lines in Figure 4a are used to obtain our best estimate of the phase behavior of symmetric blends with $\chi_{AB}N_{AVE} = 2.7$ (the same segregation strength as the asymmetric blends).

The phase behavior of the three asymmetrical blends is summarized in Figure 4b. An additional data point at $N_A/N_B = 1$ represents the results described in the preceding paragraph. At $N_A/N_B = 0.60$, we obtain lamellae at low temperatures and macrophase separation at high temperatures. Increasing N_A/N_B to 1.0 opens up a microemulsion window between the lamellar and macrophase separated states. Further increase of N_A/N_B to 3.72 results in lamellae at low temperatures, a microemulsion at intermediate temperatures, and a homogeneous phase at high temperatures. Finally increasing N_A/N_B to 18.7 leads to macrophase separation at low temperatures and a homogeneous phase at high temperatures, i.e. periodic microphases are absent. It is remarkable that the qualitatively different kinds of phase behavior reported in Figure 4b are obtained at a fixed value of $\chi_{AB}N_{AVE}$ by simply altering the relative molecular weights of the homopolymers.

Conclusions

We have studied the effect of homopolymer molecular weight asymmetry ($N_A/N_B \neq 1$) on the phase behavior of A/B/A−C blends using SANS. A series of asymmetric blends was designed to study the effect of N_A/N_B on microstructure by fixing the segregation strength of the homopolymers, and the concentration and molecular weight of the diblock copolymer. As summarized in Figure 4b, the temperature windows over which lamellae, microemulsions, macrophase separation, and homogeneous phases are found are affected qualitatively by N_A/N_B. The high temperature phase changes from a phase separated state to a homogeneous state at an N_A/N_B value between 1.0 and 3.7. Microemulsions are absent when N_A/N_B is either too small (0.6) or too large (18.7) and when they are stable, they form at intermediate temperatures with a low temperature lamellar phase. Microphase separation is entirely absent when N_A/N_B is very large (18.7). Further studies of microstructure formation in A/B/A−C blends with unequal homopolymer molecular weights seem warranted.

Acknowledgment. We acknowledge The Dow Chemical Company for providing the primary support for this work and Dr. T. H. Kalanthar for guidance and helpful discussions. A.J.N. was also supported by the Tyco Fellowship. We acknowledge the support of the National Institute of Standards and Technology, U.S. Department of Commerce, in providing the neutron research facilities used in this work. This work utilized facilities supported in part by the National Science Foundation under Agreement No. DMR-0454672.

References and Notes

(1) Reynolds, B. J.; Ruegg, M. L.; Balsara, N. P.; Radke, C. J.; Shaffer, T. D.; Lin, M. Y.; Shull, K. R.; Lohse, D. J. *Macromolecules* **2004**, *37*, 7401–7417.
(2) Lee, J. H.; Ruegg, M. L.; Balsara, N. P.; Zhu, Y. Q.; Gido, S. P.; Krishnamoorti, R.; Kim, M. H. *Macromolecules* **2003**, *36*, 6537–6548.
(3) Ruegg, M. L.; Reynolds, B. J.; Lin, M. Y.; Lohse, D. J.; Balsara, N. P. *Macromolecules* **2006**, *39*, 1125–1134.
(4) Ruegg, M. L.; Reynolds, B. J.; Lin, M. Y.; Lohse, D. J.; Balsara, N. P. *Macromolecules* **2007**, *40*, 1207–1217.
(5) Ruegg, M. L.; Reynolds, B. J.; Lin, M. Y.; Lohse, D. J.; Krishnamoorti, R.; Balsara, N. P. *Macromolecules* **2007**, *40*, 355–365.
(6) Lee, J. H.; Balsara, N. P.; Chakraborty, A. K.; Krishnamoorti, R.; Hammouda, B. *Macromolecules* **2002**, *35*, 7748–7757.
(7) Thunga, M.; Staudinger, U.; Ganss, M.; Weidisch, R.; Knoll, K. *Macromol. Chem. Phys.* **2009**, *210*, 179–188.
(8) Thunga, M.; Satapathy, B. K.; Weidisch, R.; Stamm, M.; Sommer, J. U.; Knoll, K. *Eur. Polym. J.* **2009**, *45*, 537–549.
(9) Staudinger, U.; Satapathy, B. K.; Weidisch, R. *Eur. Polym. J.* **2008**, *44*, 1822–1833.
(10) Dair, B. J.; Avgeropoulos, A.; Hadjichristidis, N.; Thomas, E. L. *J. Mater. Sci.* **2000**, *35*, 5207–5213.
(11) Meuler, A. J.; Hillmyer, M. A.; Bates, F. S. *Macromolecules* **2009**, *42*, 7221–7250.
(12) Singh, M.; Odusanya, L.; Balsara, N. P. *Abstr. Pap., Am. Chem. Soc.* **2005**, *230*, U3658–U3658.
(13) Park, M. J.; Balsara, N. P.; Jackson, A. *Macromolecules* **2009**, *42*, 6808–6815.
(14) Zhou, N.; Bates, F. S.; Lodge, T. P. *Nano Lett.* **2006**, *6*, 2354–2357.
(15) Kahlweit, M.; Strey, R.; Haase, D.; Firman, P. *Langmuir* **1988**, *4*, 785–790.
(16) Kahlweit, M.; Strey, R.; Firman, P.; Haase, D. *Langmuir* **1985**, *1*, 281–288.
(17) Kahlweit, M.; Strey, R. *Ang. Chem., Int. Ed. Engl.* **1985**, *24*, 654–668.
(18) Strey, R. *Colloid Polym. Sci.* **1994**, *272*, 1005–1019.
(19) Chen, S. H.; Choi, S. *Supramol. Sci.* **1998**, *5*, 197–206.
(20) Magid, L.; Butler, P.; Payne, K.; Strey, R. *J. Appl. Crystallogr.* **1988**, *21*, 832–834.
(21) Gompper, G.; Schick, M. *Chem. Phys. Lett.* **1989**, *163*, 475–479.
(22) Lerczak, J.; Schick, M.; Gompper, G. *Phys. Rev. A* **1992**, *46*, 985–993.
(23) Kaler, E. W.; Labourt-Ibarre, M. *Abstr. Pap. Am. Chem. Soc.* **2002**, *224*, 261-COLL.
(24) Ryan, L. D.; Schubert, K. V.; Kaler, E. W. *Langmuir* **1997**, *13*, 1510–1518.
(25) Bertrand, E.; Bonn, D.; Broseta, D.; Meunier, J. *J. Pet. Sci. Eng.* **1999**, *24*, 221–230.
(26) Adedeji, A.; Hudson, S. D.; Jamieson, A. M. *Macromolecules* **1996**, *29*, 2449–2456.
(27) Adedeji, A.; Jamieson, A. M.; Hudson, S. D. *Macromolecules* **1995**, *28*, 5255–5261.
(28) Shull, K. R.; Kellock, A. J.; Deline, V. R.; Macdonald, S. A. *J. Chem. Phys.* **1992**, *97*, 2095–2104.
(29) Robertson, M. L. Ph.D. Thesis, University of California, Berkeley, Berkeley, CA **2006**.
(30) Washburn, N. R.; Lodge, T. P.; Bates, F. S. *J. Phys. Chem. B* **2000**, *104*, 6987–6997.
(31) Holyst, R.; Schick, M. *J. Chem. Phys.* **1992**, *96*, 7728–7737.
(32) Balsara, N. P.; Fetters, L. J.; Hadjichristidis, N.; Lohse, D. J.; Han, C. C.; Graessley, W. W.; Krishnamoorti, R. *Macromolecules* **1992**, *25*, 6137–6147.
(33) Bates, F. S.; Maurer, W.; Lodge, T. P.; Schulz, M. F.; Matsen, M. W.; Almdal, K.; Mortensen, K. *Phys. Rev. Lett.* **1995**, *75*, 4429–4432.
(34) Corvazier, L.; Messe, L.; Salou, C. L. O.; Young, R. N.; Fairclough, J. P. A.; Ryan, A. J. *J. Mater. Chem.* **2001**, *11*, 2864–2874.
(35) Ellison, C. J.; Meuler, A. J.; Qin, J.; Evans, C. M.; Wolf, L. M.; Bates, F. S. *J. Phys. Chem. B* **2009**, *113*, 3726–3737.
(36) Hahn, K.; Schmitt, B. J.; Kirschey, M.; Kirste, R. G.; Salie, H.; Schmittstrecker, S. *Polymer* **1992**, *33*, 5150–5166.
(37) Jeon, H. S.; Lee, J. H.; Balsara, N. P. *Macromolecules* **1998**, *31*, 3328–3339.
(38) Hu, W. C.; Koberstein, J. T.; Lingelser, J. P.; Gallot, Y. *Macromolecules* **1995**, *28*, 5209–5214.
(39) Lin, C. C.; Jeon, H. S.; Balsara, N. P.; Hammouda, B. *J. Chem. Phys.* **1995**, *103*, 1957–1971.
(40) Lin, C. C.; Jonnalagadda, S. V.; Balsara, N. P.; Han, C. C.; Krishnamoorti, R. *Macromolecules* **1996**, *29*, 661–669.
(41) Maurer, W. W.; Bates, F. S.; Lodge, T. P.; Almdal, K.; Mortensen, K.; Fredrickson, G. H. *J. Chem. Phys.* **1998**, *108*, 2989–3000.
(42) Morkved, T. L.; Stepanek, P.; Krishnan, K.; Bates, F. S.; Lodge, T. P. *J. Chem. Phys.* **2001**, *114*, 7247–7259.
(43) Pipich, V.; Schwahn, D.; Willner, L. *Appl. Phys. a: Mater. Sci. Process.* **2002**, *74*, S345–S347.
(44) Pipich, V.; Schwahn, D.; Willner, L. *Phys. Rev. Lett.* **2005**, *94*.
(45) Pipich, V.; Schwahn, D.; Willner, L. *J. Chem. Phys.* **2005**, *123*.
(46) Pipich, V.; Willner, L.; Schwahn, D. *J. Phys. Chem. B* **2008**, *112*, 16170–16181.
(47) Schwahn, D.; Mortensen, K.; Frielinghaus, H.; Almdal, K.; Kielhorn, L. *J. Chem. Phys.* **2000**, *112*, 5454–5472.

(48) Schwahn, D.; Mortensen, K.; Frielinghaus, H.; Almdal, K. *Physica B* **2000**, *276*, 353–354.
(49) Schwahn, D.; Willner, L. *Appl. Phys. a: Mater. Sci. Process.* **2002**, *74*, S358–S360.
(50) Schwahn, D. *Phase Behavior Polym. Blends* **2005**, *183*, 1–61.
(51) Stepanek, P.; Morkved, T. L.; Krishnan, K.; Lodge, T. P.; Bates, F. S. *Phys. a: Stat. Mech. Its Appl.* **2002**, *314*, 411–418.
(52) Hillmyer, M. A.; Maurer, W. W.; Lodge, T. P.; Bates, F. S.; Almdal, K. *J. Phys. Chem. B* **1999**, *103*, 4814–4824.
(53) Bates, F. S. *Science* **1991**, *251*, 898–905.
(54) Zhou, N.; Lodge, T. P.; Bates, F. S. *J. Phys. Chem. B* **2006**, *110*, 3979–3989.
(55) Morkved, T. L.; Chapman, B. R.; Bates, F. S.; Lodge, T. P.; Stepanek, P.; Almdal, K. *Faraday Discuss.* **1999**, *112*, 335–350.
(56) Bates, F. S.; Maurer, W. W.; Lipic, P. M.; Hillmyer, M. A.; Almdal, K.; Mortensen, K.; Fredrickson, G. H.; Lodge, T. P. *Phys. Rev. Lett.* **1997**, *79*, 849–852.
(57) Leibler, L. *Makromol. Chem., Macromol. Symp.* **1988**, *16*, 1–17.
(58) Broseta, D.; Fredrickson, G. H. *J. Chem. Phys.* **1990**, *93*, 2927–2938.
(59) Kielhorn, L.; Muthukumar, M. *J. Chem. Phys.* **1997**, *107*, 5588–5608.
(60) Noolandi, J.; Hong, K. M. *Macromolecules* **1984**, *17*, 1531–1537.
(61) Fredrickson, G. H.; Bates, F. S. *J. Polym. Sci., Part B: Polym. Phys.* **1997**, *35*, 2775–2786.
(62) Duchs, D.; Ganesan, V.; Fredrickson, G. H.; Schmid, F. *Macromolecules* **2003**, *36*, 9237–9248.
(63) Certain commercial equipment, instruments, materials and suppliers are identified in this paper to foster understanding. Such identification does not imply recommendation or endorsement by the National Institute of Standards and Technology, nor does it imply that the materials or equipment identified are necessarily the best available for the purpose.
(64) Nedoma, A. J.; Robertson, M. L.; Wanakule, N. S.; Balsara, N. P. *Macromolecules* **2008**, *41*, 5773–5779.
(65) Kline, S. R. In *J. Appl. Crystallogr.*; *39*, **2006**; p 895.
(66) Temperatures are in K: $\chi_{AB} = 0.00034 + 3.94/T - 817/T^2$; $\chi_{AC} = 0.00209 - 1.18/T + 747/T^2$; $\chi_{BC} = -0.00622 + 10.6/T - 3040/T^2 + (-0.722 + 638/T - 229000/T^2)(0.2 - \phi_A)/N_{AVE,AC}$. Statistical Segment lengths: $l_A = 5.5$ Å; $l_B = 5.8$ Å; $l_C = 7.5$ Å.
(67) Flory, P. J. *J. Chem. Phys.* **1941**, *9*, 660–661.
(68) Huggins, M. L. *J. Chem. Phys.* **1941**, *9*, 440–440.
(69) Krishnamoorti, R.; Graessley, W. W.; Fetters, L. J.; Garner, R. T.; Lohse, D. J. *Macromolecules* **1995**, *28*, 1252–1259.
(70) Benoit, H.; Benmouna, M.; Wu, W. L. *Macromolecules* **1990**, *23*, 1511–1517.
(71) Akcasu, A. Z.; Tombakoglu, M. *Macromolecules* **1990**, *23*, 607–612.
(72) Balsara, N. P.; Dai, H. J. *J. Chem. Phys.* **1996**, *105*, 2942–2945.
(73) Ho, R. M.; Chiang, Y. W.; Lin, C. C.; Bai, S. J. *Macromolecules* **2002**, *35*, 1299–1306.